AIP | Applied Physics Letters

Actively controlled fibrillar friction surfaces

H. Marvi, Y. Han, and M. Sitti

Citation: Applied Physics Letters **106**, 051602 (2015); doi: 10.1063/1.4907255
View online: http://dx.doi.org/10.1063/1.4907255
View Table of Contents: http://scitation.aip.org/content/aip/journal/apl/106/5?ver=pdfcov
Published by the AIP Publishing

Actively controlled fibrillar friction surfaces

H. Marvi,[1,a)] Y. Han,[1,a)] and M. Sitti[1,2,b)]
[1]*Department of Mechanical Engineering, Carnegie Mellon University, Pittsburgh, Pennsylvania 15213, USA*
[2]*Max Planck Institute for Intelligent Systems, Heisenbergstr. 3, Stuttgart 70569, Germany*

(Received 28 September 2014; accepted 21 January 2015; published online 4 February 2015)

In this letter, we propose a technique by which we can actively adjust frictional properties of elastic fibrillar structures in different directions. Using a mesh attached to a two degree-of-freedom linear stage, we controlled the active length and the tilt angle of fibers, independently. Thus, we were able to achieve desired levels of friction forces in different directions and significantly improve passive friction anisotropies observed in the same fiber arrays. The proposed technique would allow us to readily control the friction anisotropy and the friction magnitude of fibrillar structures in any planar direction. © *2015 AIP Publishing LLC*.
[http://dx.doi.org/10.1063/1.4907255]

Adhesive and frictional properties of fibrillar surfaces inspired by gecko and insect foot-hairs have been studied for decades.[1–4] In particular, the coupling of adhesion and friction in fibrillar surfaces[5] as well as the role of fiber angle and fiber tip ending shape[6] on their frictional properties have been studied by several scientists. Murphy *et al*. showed the friction of spherical and spatula tip fibers were 1.6 and 4.7 times the maximum friction of unmodified fiber samples.[6] For frictional properties of film-terminated fibers,[7–9] it was reported that static friction of such structures increased with increasing fiber spacing as well as loading rate; however, the sliding friction was not affected by changing these factors.[8] Adhesion, friction, and wear of single-walled carbon nanotube (SWCNT) and multi-walled carbon nanotube (MWCNT) arrays were also widely studied.[10,11] Bhushan *et al*. showed that both friction and adhesion of SWCNT arrays are less than those of MWCNTs and surmised that higher stiffness of MWCNTs may contribute to their higher friction force. In another study on the frictional properties of MWCNTs, it was shown that the friction coefficient of nanotubes could significantly change depending on their orientation relative to the contact surface.[11] There are several studies suggesting different angled[6,12–15] and vertical[14–17] fibrillar structures for directional adhesion and friction properties. Murphy *et al*. measured a friction anisotropy of 5.6:1 for angled tip fibers fabricated with polyurethane,[12] a level of anisotropy similar to that observed in geckos.[5] However, the suggested designs are all passive and their frictional and adhesive properties cannot change actively. Several scientists have proposed chemical or topographical approaches for adhesion switching.[18–22] They have suggested topographical approaches such as change of backing layer stiffness[22] or using magnetic field to manipulate magnetic micropillars.[19,20] Sariola and Sitti proposed to mechanically switch adhesion for transfer printing applications using a non-adhesive mesh.[21] They retracted the fibers vertically through the mesh holes to deactivate fibrillar adhesion.[21] Most of these mechanisms take advantage of a single mechanism (e.g., tilting or retracting fibers) for switching adhesive properties of fibrillar structures. Marvi *et al*. investigated friction control mechanisms in snakes and developed a bio-inspired mechanism for active control of friction.[23–26] They controlled scale angle of attack to adjust frictional properties of Scalybot, a snake-inspired crawling robot.[26] However, there is lack of studies on active control of fibrillar friction anisotropy and magnitude, which is crucial for manipulation systems and robotic crawling and climbing systems using fibrillar structures.[27–32]

In this letter, we present a methodology through which we can actively adjust the frictional properties of fiber arrays in any planar direction by controlling the active length, L and tilt angle, θ of the fibers. As shown in Fig. 1(a), we used a mesh attached to a two degrees of freedom (2-DOF) stage to tilt the fibers (moving in y-direction in Fig. 1(b)) and change their stiffness by adjusting their active length (moving in z-direction in Fig. 1(b)). We characterized frictional properties of fibers with different tip ending shapes (Figs. 1(c)–1(f)) at different mesh configurations (Fig. 4(a)) using the setup shown in Fig. 1(b).

For the fabrication of the fibrillar surfaces used in this study (see Fig. 2), we first fabricated an acrylic mesh using an Office Mill (Haas II, OM-2A). We made an array of holes with diameters of 1 mm and center-to-center spacings of 2 mm in an acrylic plate of thickness 6.3 mm. We then silanized the mesh to reduce the surface energy of acrylic and made a backing layer for it. Next, we poured ST-1087 polyurethane (BJB Enterprises, Inc., mixed 100:50 by weight) on this mesh to fabricate master fibers. We used a piece of cured Dow Corning HS-II silicon rubber (mixed 10:1 by weight) to remove the excess polymer from the top of mesh. We left the silicon rubber on top of the mesh until the polyurethane cured in order to get uniform fiber tips illustrated in Fig. 1(c). According to scanning electron microscope (SEM) images taken from the cross section of these fiber tips, the maximum height difference on each fiber tip (height at the tip edge minus height at its center) normalized by the fiber diameter was 0.066 ± 0.007. The ratio of tip to stem diameter was also 1.00. Next, we made a mold from these fibers using silicon rubber and used ST-1060 polyurethane (BJB

[a)]H. Marvi and Y. Han contributed equally to this work.
[b)]Author to whom correspondence should be addressed. Electronic mail: sitti@is.mpg.de

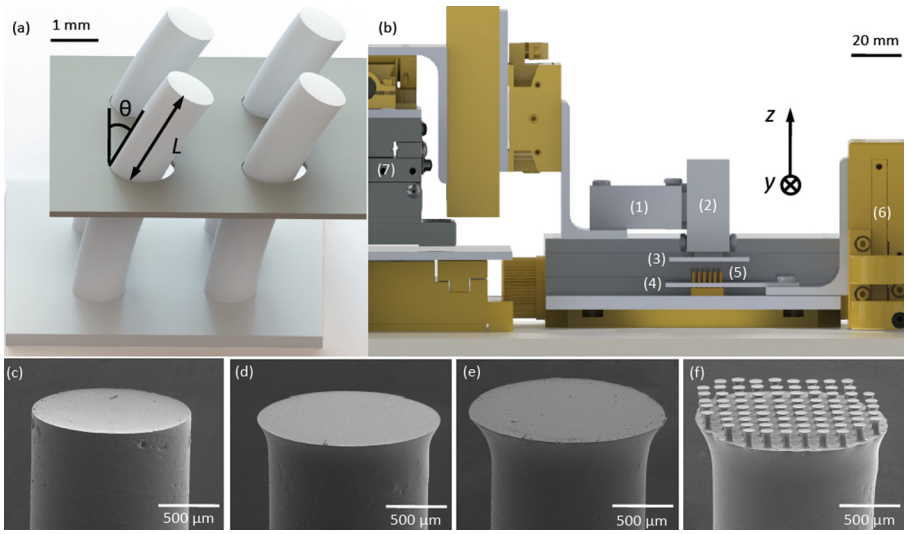

FIG. 1. (a) Schematic of active fiber friction anisotropy and magnitude control. We used a 2-DOF linear stage to change fiber array active length, L (moving the mesh in the z-direction) and its tilt angle, θ (moving the mesh in the y-direction). (b) Friction measurement setup: (1) 50 g load cell for normal load, (2) 500 g load cell for shear load, (3) flat glass indenter, (4) mesh, (5) fiber array, (6) 2-DOF linear manual stage, and (7) 3-DOF linear motorized stage. SEM images of fibers used in this study with different tip decorations: (c) undecorated tip, (d) small mushroom tip, (e) large mushroom tip, and (f) hierarchical fibers. These fibers are all made of ST-1060 polyurethane.

Enterprises, Inc., mixed 100:55 by weight) to fabricate fibers using this mold.

We decorated tips of these fibers in three different ways (see Figs. 1(d)–1(f)): small and large mushroom tip fibers and hierarchical fibers. For fabricating small mushroom tip fibers, we spin coated 0.2 g of ST-1060 at 2000 rpm for 60 s, dipped the undecorated fiber array in the thin layer of polyurethane, and cured it while being pressed on a flat surface made of silicon rubber (see Fig. 3). The ratio of tip to stem diameter was 1.17 ± 0.02. We used the same procedure for fabricating large mushroom tips unless we spin coated 0.2 g of ST-1060 at 1500 rpm for 45 s. The ratio of tip to stem diameter for large mushroom tips was 1.26 ± 0.02. For making hierarchical fibers, we spin coated 0.2 g of ST-1060 at 2000 rpm for 60 s and dipped the undecorated fiber array in the thin layer of polyurethane and let the polymer be cured while being pushed against a flat surface made of silicon rubber. We then spin coated 0.2 g of ST-1060 at 1500 rpm for 45 s and dipped the fiber array in the thin layer of polyurethane and cured it while pressing it against a mold previously developed for small mushroom tip fibers (stem diameter of 40 μm, tip diameter of 90 μm, and length of 100 μm).[21] Finally, we made a silicon rubber mold for each tip decoration to be able to make consistent fibers for our friction measurements. The curing procedures we followed for polymers we used in this study are as follows: we cured ST-1060 and ST-1087 fibers for 24 h at room temperature followed by 16 h at 71 °C. We also cured silicon rubber for 24 h at room temperature. We degassed polymers 3 min after mixing and 10 min after pouring them on the mold.

We performed our friction tests on four different fiber tips (undecorated tip, small mushroom tip, large mushroom tip, and hierarchical fibers as illustrated in Figs. 1(c)–1(f) using the setup shown in Fig. 1(b).[33] We used a laser engraver (CO_2, 35 W, Pinnacle V-series) to fabricate a mesh made of 1.5 mm thick acrylic with holes of 1.5 mm diameter spaced at 2 mm. We attached this mesh to a 2-DOF manual micro-manipulator stage to adjust the active length and tilt angle of fibers (Fig. 1(b)). We first fixed the sample on a glass slide using double-sided tape and hot glue around the edges. We then aligned the mesh with the fibers and moved it down until it contacted the backing layer. We used a flat glass indenter for all of the friction tests. We attached this indenter to the shear force load cell, which was attached to the $z-y$ motorized stage through the normal force load cell (Fig. 1(b)). Next, we used the two rotational DOF of the stage to align the indenter with fibers. Once we did the alignment, we approached the fibers at speed of 0.05 mm/s, preloaded them

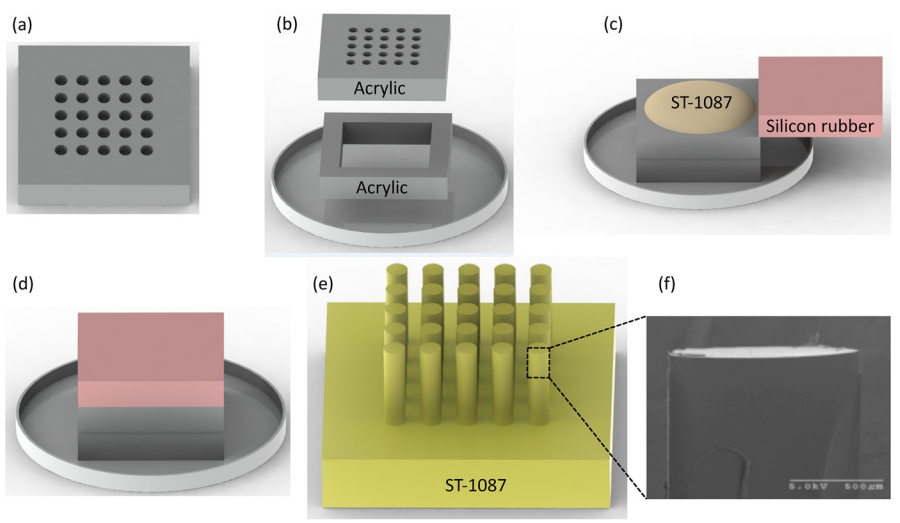

FIG. 2. Fabrication steps of master fibers: (a) making the acrylic mesh using an office mill. Holes have diameter of 1 mm and center-to-center spacing of 2 mm. The thickness of acrylic plate is also 6.3 mm. (b) Using superglue to attach the mesh to an acrylic backing layer and to attach the backing layer to a petri dish. (c) Pouring ST-1087 polyurethane on the mesh and removing extra material from the top of mesh using a piece of cured Dow Corning HS-II silicon rubber. (d) Curing the ST-1087 polyurethane while the silicon rubber is on the mesh. (e) Peeling the master fiber out of the mesh. (f) SEM image of fiber tip cross section.

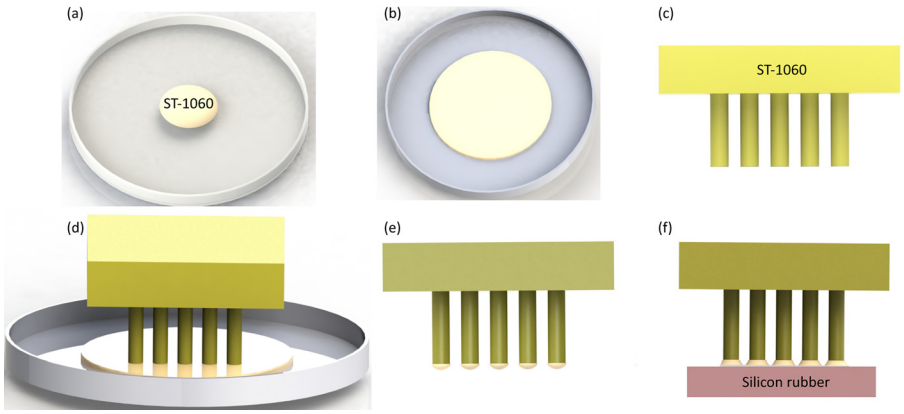

FIG. 3. Fabrication process for mushroom tip fibers: (a) and (b) Pouring 0.2 g of ST-1060 in a petri dish and spin coating it at 1500 rpm for 45 s. (c) and (d) Dipping the fiber array in the thin layer of ST-1060 polyurethane. (e) and (f) Pressing the fiber tips against a flat piece of cured silicon rubber and curing it.

with 0.25 N normal load, contacted the fibers for 10 s, dragged the indenter on the fiber array at speed of 0.1 mm/s for 10 mm, and finally retracted the indenter. Once the indenter made contact with fibers and we applied the preload, the indenter height was kept constant to measure friction force at constant z-distance between fibers and glass indenter. See supplementary Figs. S1(a)-S1(c) for the raw friction data and Figs. S1(d) and S1(e) for the effect of normal load and drag speed on the highest static friction force experienced by the undecorated fibers.[34]

We performed a total of 96 trials using four different samples (one sample per tip decoration), with and against fiber tilt angles, at four different configurations of the mesh ($z=0$, 3 mm according to active fiber length of 4.6 mm and 1.6 mm considering the thickness of the mesh and $y=0$, 2 mm; Fig. 4(a), configurations 1–4), three trials each. Figures 4(b)–4(e) present the highest static friction force as a function of fiber active length and angle (according to different $z-y$ levels of the mesh) for the four different samples we used in this study. Figures 4(f)–4(i) were similarly plotted using the kinetic friction force of these samples. The friction force was measured in two opposing directions: with (red bars) and against (blue bars) the direction of fiber tilt angle to find the level of friction anisotropy achieved in different $z-y$ levels. We adjusted the alignment of the setup by minimizing the static friction anisotropy of vertical fibers ($y=0$).

The frictional properties of fibers in this study were impacted by both adjusting their effective lengths and tilting them. We first look at the effect of tilting the fibers, then shortening them, and finally the combined effect of these

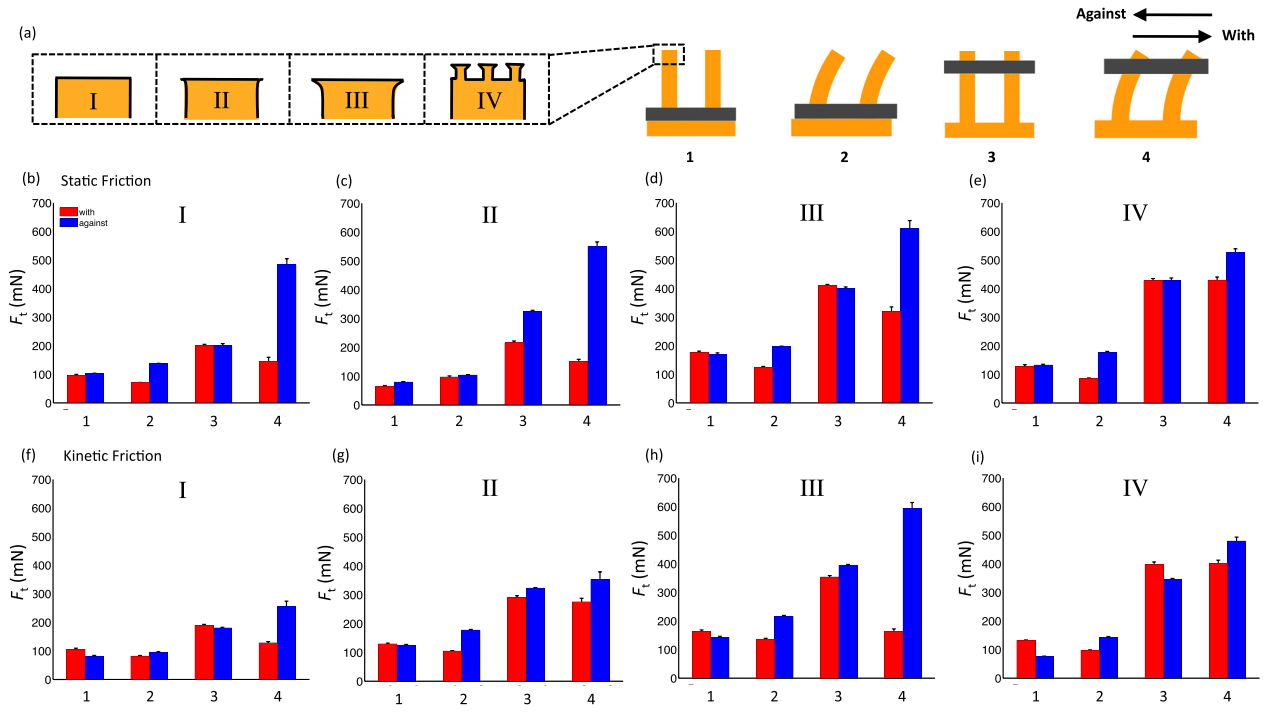

FIG. 4. (a) Different mesh positions (1–4) and fiber tip ending shapes (I–IV). Highest static friction force as a function of $z-y$ level of the mesh in "with" and "against" directions for (b) undecorated tip, (c) small mushroom tip, (d) large mushroom tip, and (e) hierarchical fibers. Kinetic friction force as a function of $z-y$ level of the mesh in "with" and "against" directions for (f) undecorated tip, (g) small mushroom tip, (h) large mushroom tip, and (i) hierarchical fibers. Comparing friction data for configurations 1 and 3 demonstrate the effect of fiber array active length on its frictional properties. The shorter the fiber was, the higher the friction force was. The differences in friction forces between configurations 1 and 2 and between configurations 3 and 4 are due to tilting fibers. The "with" friction was decreased and "against" friction was increased due to tilting fibers. Comparing configurations 1 and 4 shows the effect of both mechanisms: changing fiber length and tilting it. These experiments were performed under constant z distance between fiber array and glass indenter (after applying the preload the indenter height was kept constant).

mechanisms. As shown in Fig. 1(a), tilting the fibers using the mesh would cause both the fiber stem and fiber tip to tilt where each of these effects would result in friction anisotropy.[12] As supported by most of the data plotted in Figs. 4(b)–4(i), tilting the fibers decreased both their static and kinetic friction in the "with" direction while increasing friction in the "against" direction, when compared to vertical fibers. The role of angle of attack on adjusting backward to forward friction anisotropy of snake-inspired scales has been studied by Marvi *et al*.[26] They used aluminum blades as scales and changed their angles of attack to actively control frictional anisotropy on Styrofoam and achieved static friction anisotropy of 2.16 and kinetic friction anisotropy of 1.6.[26]

If we only look at the effect of fiber shortening, the shorter the fiber length, the higher the static and kinetic friction force due to higher fiber stiffness. In a similar observation, Bhushan *et al*. showed that the friction of SWCNT arrays is less than that of the stiffer MWCNTs.[10] Due to the combined effect of fiber shortening and tilting on increasing "against" friction force, the highest static and kinetic friction forces for each sample were measured by dragging in the "against" direction at configuration 4 (short and tilted fibers, see Fig. 4(a)).

The four different samples we used in this study all revealed similar trends as discussed in the previous paragraph. However, large mushroom tip fibers demonstrated the highest static and kinetic friction forces of 608.77 $\pm$ 28.90 and 593.66 $\pm$ 20.64 mN, respectively, with 250 mN preload. This is mainly due to the larger area of contact and higher adhesion of mushroom tip fibers. The effect of tip decoration on frictional properties of fibrillar structures was studied by Murphy *et al*. who measured higher friction forces for spherical and spatula tip fibers compared to unmodified fiber samples.[6] The highest kinetic friction anisotropy is also observed in the mushroom tip sample (1:3.6). However, small mushroom tip fibers showed the highest static friction anisotropy (1:3.7).

Following the proposed methodology, we can change the effective length of fibers and their tilt angles both of which contribute to the frictional properties of the fibers. Thus, we can adjust the "with" and "against" friction forces readily. As an illustration, if we fabricate passive large mushroom tip fiber arrays in configuration 4, we could only achieve static friction anisotropy of 1:1.9. However, using the proposed technique, we could improve the friction anisotropy of this fiber array to 1:4.9 if we use configuration 2 for "with" direction and configuration 4 for "against" direction. We can also reverse the "with" and "against" direction of fibers by tilting the fiber array in the opposite direction. Moreover, we can extend this mechanism to any arbitrary planar direction or deactivate the fiber array friction by reducing its effective length to zero. Thus, we can have a fibrillar surface that could adapt to the environment and actively adjust its frictional properties in different directions.

Making effective interactions with the environment using attachment mechanisms that could adapt to the terrain and gait requirements could make locomotion on unstructured complex terrain feasible. Incorporating the proposed mechanism in a terrestrial robotic system could allow the robot to adjust its frictional properties in any planar direction and make more effective interactions with its surrounding environment. However, there are several limitations on the proposed methodology. Having such a mechanism would require adding several actuators to the robotic system. Moreover, the frictional properties of these fibrillar structures are characterized on a flat glass indenter. In order to come up with an optimum fiber design and control strategy for such an application, further friction characterization on different surfaces will be required (depending on the terrain the robot will be traversing). It should also be emphasized that the mesh configurations used in this study are not the optimal positions of z and y for maximum friction anisotropy and were arbitrarily chosen to demonstrate the effectiveness of the proposed methodology.

In summary, we proposed a technique for active control of frictional properties of fibrillar structures. We used a 2-DOF linear stage to control the fiber length and the tilt angle in order to adjust its friction forces in different directions. We used four different samples for our experiments and performed friction measurements in "with" and "against" directions for four different configurations of the mesh. According to our measurements, both length and tilt angle contributed to the friction forces experienced by fibers. Tilting the fibers decreased their friction force in "with" direction and increased it in "against" direction compared to those of vertical fibers. In addition, decreasing the effective fiber length increased its friction force in both directions. The large mushroom tip fibers demonstrated superior frictional properties in this study. We also showed how we can use this technique to improve the static friction anisotropy of large mushroom tip fibers 2.6 times the maximum anisotropy such passive structure could have. The methodology proposed in this study would allow us to actively control friction forces of fibrillar structures in any planar direction or remove fibrillar friction if needed. Active control of friction would enable pick-and-place type of robotic manipulation and transfer printing systems for flexible electronics and miniature electronic, optical,[35–37] and mechanical device assembly and packaging applications[21,27,28] and snake, gecko, or other biologically inspired robotic crawling and climbing systems,[29–32] which could traverse various surfaces and terrain by active friction control for search and rescue, exploration, inspection, and field robotics applications.

The authors thank V. Sariola and U. Abusomwan for invaluable discussions and review of our manuscript, J. Suhan for the SEM micrographs, National Science Foundation (NSF CMMI-1130520) for funding, and members of the NanoRobotics Laboratory for helpful comments.

[1]K. Autumn, Y. A. Liang, S. T. Hsieh, W. Zesch, W. P. Chan, T. W. Kenny, R. Fearing, and R. J. Full, Nature **405**, 681 (2000).
[2]K. Autumn, M. Sitti, Y. A. Liang, A. M. Peattie, W. R. Hansen, S. Sponberg, T. W. Kenny, R. Fearing, J. N. Israelachvili, and R. J. Full, Proc. Natl. Acad. Sci. U.S.A. **99**, 12252 (2002).
[3]Y. Tian, N. Pesika, H. Zeng, K. Rosenberg, B. Zhao, P. McGuiggan, K. Autumn, and J. Israelachvili, Proc. Natl. Acad. Sci. U.S.A. **103**, 19320 (2006).
[4]M. Zhou, N. Pesika, H. Zeng, Y. Tian, and J. Israelachvili, Friction **1**, 114 (2013).
[5]K. Autumn, A. Dittmore, D. Santos, M. Spenko, and M. Cutkosky, J. Exp. Biol. **209**, 3569 (2006).

[6]M. P. Murphy, B. Aksak, and M. Sitti, J. Adhes. Sci. Technol. **21**, 1281 (2007).
[7]L. Shen, N. J. Glassmaker, A. Jagota, and C. Y. Hui, Soft Matter **4**, 618 (2008).
[8]L. Shen, A. Jagota, and C. Y. Hui, Langmuir **25**, 2772 (2009).
[9]S. Vajpayee, R. Long, L. Shen, A. Jagota, and C. Y. Hui, Langmuir **25**, 2765 (2009).
[10]B. Bhushan, B. Galasso, C. Bignardi, C. V. Nguyen, L. Dai, and L. Qu, Nanotechnology **19**, 125702 (2008).
[11]P. Dickrell, S. Sinnott, D. Hahn, N. Raravikar, L. Schadler, P. Ajayan, and W. Sawyer, Tribol. Lett. **18**, 59 (2005).
[12]M. P. Murphy, B. Aksak, and M. Sitti, Small **5**, 170 (2009).
[13]J. Lee, R. S. Fearing, and K. Komvopoulos, Appl. Phys. Lett. **93**, 191910 (2008).
[14]D. Sameoto and C. Menon, Smart Mater. Struct. **19**, 103001 (2010).
[15]M. K. Kwak, C. Pang, H. E. Jeong, H. N. Kim, H. Yoon, H. S. Jung, and K. Y. Suh, Adv. Funct. Mater. **21**, 3606 (2011).
[16]J. Tamelier, S. Chary, and K. L. Turner, Langmuir **28**, 8746 (2012).
[17]D. Sameoto, H. Sharif, J. P. Diaz Tellez, B. Ferguson, and C. Menon, J. Adhes. Sci. Technol. **28**, 354 (2014).
[18]M. Kamperman and A. Synytska, J. Mater. Chem. **22**, 19390 (2012).
[19]D. M. Drotlef, P. Blumler, and A. del Campo, Adv. Mater. **26**, 775 (2014).
[20]M. T. Northen, C. Greiner, E. Arzt, and K. L. Turner, Adv. Mater. **20**, 3905 (2008).
[21]V. Sariola and M. Sitti, Adv. Mater. Interfaces **1**, 1300159 (2014).
[22]J. Krahn, D. Sameoto, and C. Menon, Smart Mater. Struct. **20**, 015014 (2011).
[23]H. Marvi, Ph.D. dissertation, Georgia Institute of Technology, 2013.
[24]H. Marvi and D. L. Hu, J. R. Soc. Interface **9**, 3067 (2012).
[25]H. Marvi, J. Bridges, and D. L. Hu, J. R. Soc. Interface **10**, 20130188 (2013).
[26]H. Marvi, G. Meyers, G. Russell, and D. L. Hu, in *Proceedings of ASME Dynamic Systems and Control Conference* (2011), p. 443.
[27]Y. Menguc, S. Y. Yang, S. Kim, J. A. Rogers, and M. Sitti, Adv. Funct. Mater. **22**, 1246 (2012).
[28]S. Song and M. Sitti, Adv. Mater. **26**, 4901 (2014).
[29]M. P. Murphy, C. Kute, Y. Menguc, and M. Sitti, Int. J. Rob. Res. **30**, 118 (2011).
[30]S. Kim, M. Spenko, S. Trujillo, B. Heyneman, D. Santos, and M. R. Cutkosky, IEEE Trans. Rob. **24**(1), 65 (2008).
[31]D. Santos, M. Spenko, A. Parness, S. Kim, and M. Cutkosky, J. Adhes. Sci. Technol. **21**, 1317 (2007).
[32]D. Santos, B. Heyneman, S. Kim, N. Esparza, and M. R. Cutkosky, in *Proceedings of IEEE International Conference on Robotics and Automation* (2008), p. 1125.
[33]B. Aksak, C. Y. Hui, and M. Sitti, J. R. Soc. Interface **8**, 1166 (2011).
[34]See supplementary material at http://dx.doi.org/10.1063/1.4907255 for raw friction data and the effect of normal load and drag speed on the highest static friction force experienced by the undecorated fibers.
[35]X. Lin, T. Ling, H. Subbaraman, X. Zhang, K. Byun, L. J. Guo, and R. T. Chen, Opt. Lett. **38**, 1597 (2013).
[36]X. Zhang, A. Hosseini, X. Lin, H. Subbaraman, and R. T. Chen, IEEE J. Sel. Top. Quantum Electron. **19**, 3401115 (2013).
[37]H. Subbaraman, D. T. Pham, X. Xu, M. Y. Chen, A. Hosseini, X. Lu, and R. T. Chen, IEEE Antennas Wireless Propag. Lett. **12**, 170 (2013).